Positive Inotropic Effects of Low dATP/ATP Ratios on Mechanics and Kinetics of Porcine Cardiac Muscle

Brenda Schoffstall,*† Amanda Clark,† and P. Bryant Chase*†‡
*Program in Molecular Biophysics, †Department of Biological Science, and ‡Department of Chemical & Biomedical Engineering, Florida State University, Tallahassee, Florida

ABSTRACT Substitution of 2′-deoxy ATP (dATP) for ATP as substrate for actomyosin results in significant enhancement of in vitro parameters of cardiac contraction. To determine the minimal ratio of dATP/ATP (constant total NTP) that significantly enhances cardiac contractility and obtain greater understanding of how dATP substitution results in contractile enhancement, we varied dATP/ATP ratio in porcine cardiac muscle preparations. At maximum Ca^{2+} (pCa 4.5), isometric force increased linearly with dATP/ATP ratio, but at submaximal Ca^{2+} (pCa 5.5) this relationship was nonlinear, with the nonlinearity evident at 2–20% dATP; force increased significantly with only 10% of substrate as dATP. The rate of tension redevelopment (k_{TR}) increased with dATP at all Ca^{2+} levels. k_{TR} increased linearly with dATP/ATP ratio at pCa 4.5 and 5.5. Unregulated actin-activated Mg-NTPase rates and actin sliding speed linearly increased with the dATP/ATP ratio ($p < 0.01$ at 10% dATP). Together these data suggest cardiac contractility is enhanced when only 10% of the contractile substrate is dATP. Our results imply that relatively small (but supraphysiological) levels of dATP increase the number of strongly attached, force-producing actomyosin cross-bridges, resulting in an increase in overall contractility through both thin filament activation and kinetic shortening of the actomyosin cross-bridge cycle.

INTRODUCTION

Cardiac contractility can be enhanced by a variety of mechanisms, including those that directly affect actomyosin interactions. One such positive inotropic effector that acts primarily via actomyosin is replacement of ATP by 2′-deoxy ATP (dATP) as substrate for cardiac muscle contraction (1). With both α-myosin heavy chain (α-MHC, fast isoform) from untreated rats and β-myosin heavy chain (β-MHC, slow isoform) from propylthiouracil (PTU) treated rats, replacement of ATP with dATP as the substrate for cardiac contraction resulted in significant increases of contractile parameters (1). The effects of this substrate substitution on mechanical properties were evaluated with isometric force (F_{iso}), rate of tension redevelopment (k_{TR}), unloaded shortening velocity (V_{us}) at maximum activating [Ca^{2+}], as well as unregulated NTP hydrolytic activity (Mg-NTPase) and in vitro motility (IVM) actin sliding speed; all parameters were significantly enhanced in rat cardiac muscle, and these effects are larger than in skeletal muscle (2–4). From these results it is evident that dATP as substrate increases the number of strongly attached, force-producing actomyosin cross-bridges. However, it is not structurally clear why the removal of one oxygen from the ATP structure should cause a change in myosin activity and the actomyosin force generating cycle. Although studies have indicated that ATP and dATP have a similar binding affinity for myosin (1), it is possible that the K_m of dATP for myosin is lower than that of ATP, which could lead to higher affinity of myosin for dATP. An overall enhancement of actomyosin kinetics with dATP may result in a shorter cross-bridge cycle. Cardiac contractility may be thus enhanced both by greater numbers of strong cross-bridges and a faster cross-bridge cycle when dATP is utilized as contractile substrate.

To understand which properties of cardiac thin filament activation can be limiting to contraction, Regnier et al. investigated F_{iso} and k_{TR} utilizing dATP as an analog of ATP for in vitro assays with rat cardiac trabeculae (5). This study showed that dATP as contractile substrate increased the Ca^{2+} sensitivity of both F_{iso} and k_{TR} and increased both force and k_{TR} at maximum activating Ca^{2+}. The force-k_{TR} relation was unaltered at lower levels of steady-state force but was extended to higher force and k_{TR} with dATP for both the α- and β-MHC rat cardiac isoforms. This led to the conclusion that even at saturating Ca^{2+}, thin filament Ca^{2+} activation may limit the rate of force development in rat cardiac muscle (5). If dATP increases the number of strong cross-bridges, cross-bridge enhancement of thin filament activation could become prominent in cardiac contraction at all levels of Ca^{2+} activation (6). This mechanism is plausible because *N*-ethyl-maleimide myosin subfragment 1 (NEM-S1), a long-lived analog of a strongly bound cross-bridge in the presence of NTP, increases k_{TR} at submaximal Ca^{2+} levels that can reach or exceed the rate normally achieved at maximum Ca^{2+} activation (7). Because Ca^{2+} activation is limiting under normal conditions as well as heart failure conditions, there is a maximum increase in contractile parameters that occurs with increasing intracellular [Ca^{2+}]. However, the rat cardiac trabeculae studies indicate that cardiac

Submitted December 2, 2005, and accepted for publication June 8, 2006.

Address reprint requests to P. Bryant Chase, PhD, F.A.H.A. Dept. of Biological Science, Florida State University, Biology Unit One, Tallahassee, FL. 32306. Tel.: 850-644-0056; Fax: 850-644-0481; E-mail: chase@bio.fsu.edu.

© 2006 by the Biophysical Society

0006-3495/06/09/2216/11 $2.00

doi: 10.1529/biophysj.105.079061

contraction can be further enhanced with dATP as contractile substrate due to the increased numbers of strong force-producing cross-bridges that activate the thin filament above that normally achievable at high [Ca^{2+}] (5).

In addition to thin filament activation by increased numbers of strongly attached cross-bridges, it is possible that the enhanced force-pCa relationship found with dATP as contractile substrate is partially due to increased duty ratio. The increased duty ratio may be a result of a shorter overall cross-bridge cycle and an increased affinity of dATP for myosin over that of ATP. This assumption is reasonably inferred from the effects of dATP on rat cardiac contraction in unregulated in vitro assays (1) without the influence of the thin filament regulatory proteins. Microneedle assays measuring steady-state force generated on individual unregulated actin filaments interacting with a rabbit skeletal HMM (heavy meromyosin) coated surface showed that mean force per filament length was increased by approximately threefold when dATP was substituted for ATP as contractile substrate (8); an increased actomyosin duty ratio may account for this effect.

To date, all studies utilizing dATP as substrate in vitro have completely replaced ATP with dATP. It is therefore of interest to know if a small increase in the dATP/ATP ratio can significantly enhance cardiac contractility. Increased dATP in vivo has potential as a therapeutic intervention for the symptoms of heart failure because its positive inotropic action would be through a direct effect on the myofilaments (1,9). To determine the smallest dATP/ATP ratio that can significantly enhance in vitro cardiac contractility, we explored the effects of increasing ratios of dATP/ATP (constant total [NTP]) on cardiac muscle contraction. We also investigated the hypothesis that dATP affects cardiac contraction primarily via recruitment of strong actomyosin cross-bridges and examined the possibility that dATP increases duty ratio while shortening the cross-bridge cycle. Previous studies with dATP utilized rat cardiac muscle preparations. We used porcine cardiac muscle as our model because the β-MHC isoform in pigs is kinetically more like human cardiac β-MHC isoform than that in rodents (10).

Here we test the hypothesis that a relatively small ratio of dATP/ATP (but greater than physiological) can significantly enhance contractile parameters and actomyosin cross-bridge cycling, manifested as the combination of higher numbers of strongly attached force-producing cross-bridges, increased NTP hydrolysis rate, increased rate of myosin head attachment, and increased rate of myosin head detachment. We predicted that these effects would substantiate previous evidence that strong cross-bridge binding can significantly increase force by enhancement of activation of the thin filament in cardiac muscle and that dATP as substrate causes an enhancement of in vitro indicators of contractility. To test our hypothesis we first characterized the force-pCa relationship with permeabilized porcine cardiac papillary muscle fiber bundles, utilizing either 100% ATP or 100% dATP as contractile substrate. Next, we measured steady-state force and k_{TR} in porcine cardiac fiber bundles as the ratio of dATP/ATP was increased with a constant total NTP concentration. To investigate effects on the cross-bridge cycle, we compared unregulated actin-activated Mg-NTPase rates and unregulated actin sliding speeds (with IVM) as ratios of dATP/ATP were increased (constant total [NTP]) utilizing porcine cardiac myosin (pcMyosin).

We found that porcine cardiac F_{iso} was increased at pCa $\leq$ 5.7 when dATP replaced ATP, and pCa_{50} was unchanged. At maximum Ca^{2+} (pCa 4.5) F_{iso} increased linearly with dATP/ATP ratio, but at submaximal Ca^{2+} (pCa 5.5) this relationship was nonlinear. The increase in F_{iso} was highly significant when as little as 10% dATP (90% ATP) was present. k_{TR} increased with dATP at all levels of Ca^{2+} activation and increased linearly with an increase in the dATP/ATP ratio. Actin-activated Mg-NTPase rate as well as unregulated actin sliding speed with pcMyosin increased linearly with dATP/ATP ratio; actin sliding speed was significantly increased with only 10% dATP/ATP. Together these data suggest that the cardiac contractility with the porcine β-MHC isoform is increased when at least 10% of the contractile substrate is dATP and that dATP increases the actomyosin duty ratio while shortening the overall cross-bridge cycle. In addition, an increase in the number of strongly attached cross-bridges with dATP enhances activation of the thin filament for an overall increase in contractility.

Preliminary abstracts of this work have been published (11,12).

METHODS

Rabbit skeletal muscle actin

Male New Zealand White rabbits were handled in accordance with the current National Institutes of Health/National Research Council *Guide for the Care and Use of Laboratory Animals*. All procedures and protocols were approved by Florida State University's Institutional Animal Care and Use Committee. Actin used in the motility and Mg-Mg-NTPase assays was extracted from acetone powder prepared from New Zealand White rabbit back and leg muscles (13,14). Proteins are routinely analyzed by sodium dodecyl sulfate-polyacrylamide gel electrophoresis (SDS-PAGE).

Porcine cardiac muscle preparations

Porcine hearts were obtained from a local abattoir within 20 min of the animal's death.

Skinned papillary muscle strips

For fiber mechanics, hearts were temporarily stored in oxygenated Ringer's solution (116 mM NaCl, 4.6 mM KCl, 1.16 mM KH_2PO_4, 25.3 mM $NaHCO_3$, 2.5 mM $CaCl_2$, and 1.16 mM $MgSO_4$) on ice for transport to the laboratory, where the cardiac papillary muscles were immediately dissected. Muscle strips ~3–5 mm in diameter and 5 mm in length were sectioned from the left ventricle papillary muscle, then tied to Teflon strips for storage. The strips were skinned in a 1% Triton X-100 relaxing (pCa 8) solution for 24 h at 4°C. The strips were rinsed, then stored in a 50% v/v glycerol-pCa 8 solution at −20°C (15). Small bundles of permeabilized muscle from these strips were used within 1 month after dissection.

Purified cardiac myosin

For pcMyosin used in the IVM assays and actin-activated Mg-NTPase assays, fresh porcine hearts were rinsed in ice cold phosphate buffer saline (PBS) (137 mM NaCl, 2.7 mM KCl, 10 mM Na_2HPO_4, 1.8 mM KH_2PO_4) to remove residual blood, and the atria were removed. The ventricles were transported in cold buffer consisting of 25 mM Na_2EGTA, 50 mM MOPS 3-((*N*-morpholino)propanesulfonic acid), 6 mM $MgCl_2$, 4 mM acetic acid, 5.5 mM ATP, 2 mM DTT (1,4-dithiothreitol), 50 μg/ml leupeptin, 1 μg/ml pepstatin A, 0.2 mM phenylmethylsulfonylfluoride (PMSF), and Complete Protease inhibitor cocktail (Roche Diagnostics, Mannheim, Germany), pH 6.8, maintained on ice. Ventricles were ground in a cold meat grinder, and 50–75 g of tissue was homogenized in 400 ml of buffer A. Buffer A consisted of 0.3 M KCl, 10 mM $Na_4P_2O_7$, 1 mM $MgCl_2$, 20 mM DTT, 5 mM EGTA, 150 mM K_2HPO_4, 5 μg/ml leupeptin, 0.7 μg/ml pepstatin A, 0.2 mM PMSF, pH 6.8. pcMyosin was extracted from this tissue homogenate, filtered, diluted with 20 vol cold 1 mM DTT, and allowed to precipitate overnight at 4°C. The pcMyosin precipitate was pelleted and then resuspended in 0.3 M KCl, 10 mM imidazole, 5 mM $MgCl_2$, 20 mM DTT, 10 mM ATP, 5 μg/ml leupeptin, 0.7 μg/ml pepstatin A, pH 6.8. This resuspension was centrifuged at 19,000 rpm (SS-34 rotor) for 30 min to remove insoluble actin. The supernatant was diluted with 8 vol of cold 1 mM DTT and allowed to precipitate for 3 h. The pcMyosin precipitate was pelleted and resuspended in 0.6 M KCl, 2 mM $MgCl_2$, 5 mM DTT, 10 mM Tris-HCl, and Complete Protease inhibitor cocktail, pH 7.6, then stored in 50% glycerol (v/v).

To prepare the glycerinated pcMyosin for use in most motility assays, the glycerol stock was precipitated with a bicarbonate buffer consisting of 0.1 mM $NaHCO_3$ and 0.1 mM EGTA, then centrifuged to form a pellet. The pellet was resuspended in 11.4 mM imidazole-HCl, 0.67 M KCl, 2.3 mM $MgCl_2$, 0.04 mM $NaHCO_3$, 0.04 mM EGTA, and concentration of pcMyosin was determined by a modified Bradford assay (Pierce Biotechnology, Rockford, IL). Bicarbonate buffer with 3 μM $MgCl_2$ was added to this solution at 1.2 ml/mg of pcMyosin. After centrifugation to remove any precipitated pcMyosin and actin, the concentration of the resulting pcMyosin preparation in solution was determined. For studies where high concentrations of pcMyosin were needed to compare motility at different pcMyosin densities, the pellets were resuspended in 0.3 M KCl, 25 mM imidazole, 1 mM EGTA, 4 mM $MgCl_2$, and 10 mM DTT (16). In both cases, prepared pcMyosin was treated with equimolar actin and 1 mM ATP and then centrifuged to remove dead heads. Although the majority of dead heads were removed at this step, a small proportion of dead heads remained in the preparation due to the salt concentration necessary to keep pcMyosin in solution.

To prepare the pcMyosin for Mg-NTPase analysis, glycerinated stock was precipitated with a bicarbonate buffer consisting of 0.1 mM $NaHCO_3$ and 0.1 mM EGTA and then centrifuged. The pellet was resuspended in Mg-NTPase buffer consisting of 1 mM DTT, 5 mM $MgCl_2$, 1 mM EGTA, 25 mM Tris (pH 7.0), and 0.3 M KCl; 0.1 M stocks of ATP and dATP were mixed in designated ratios of dATP/ATP.

Fiber mechanics

Mounting of glycerinated porcine papillary fibers

For experiments, small fiber bundles were separated from glycerinated muscle strips, and the ends were wrapped in aluminum foil T-clips for attachment to the force transducer via small wire hooks. Fiber bundles were mounted on a motor (step time 300 μs) (Aurora Scientific, Ontario, Canada) to control overall fiber length at one end, and on a capacitative-type force transducer ($f_c = 3.3$ kHz; Aurora Scientific) at the other end. The motor and force transducer were located on a modified stage of an inverted microscope (17). L_0 was determined and set by reducing passive tension at pCa 9 to zero baseline before the start of each experiment. Fiber length and fiber diameter (measured with an optical micrometer) were measured before the start of each experiment. Fiber bundles were 243 ± 39 μm wide and 1.5 ± 0.3 mm long ($n = 15$).

Experimental control, data acquisition, and data analysis

Steady-state isometric force and the kinetics of tension redevelopment (k_{TR}) were determined as described previously (14,18,19). k_{TR} was obtained after recording steady-state isometric force by applying a rapid shortening, then restretch to original fiber length (14). The experimental control system employed periodic (0.2 Hz) unloading (i.e., ~15% original length (L_0) fiber shortening followed by restretch to L_0). Force was digitized and analyzed using custom data acquisition and control software (20). All signals were low-pass filtered (CyberAmp 380, Axon Instruments, Foster City, CA) to avoid aliasing. Steady-state isometric force was measured with the capacitative-type force transducer. In all experiments, fibers were moved rapidly between solutions of varying pCa and/or varying dATP/ATP concentrations. Experimental solutions were held in 100- or 200-μl anodized aluminum wells. The bottom of each well consisted of a glass No. 1 thickness coverslip. The temperature of the wells was set at 15°C and controlled to within 1°C during individual experiments using an ATR-4 adaptable thermoregulator (Quest Scientific, North Vancouver, BC, Canada). Reduced temperature (15°C) and length cycling were utilized to maintain integrity of fiber structure and mechanical properties during prolonged activation. Measurements of total force were obtained from the initial portion of digitized records in which the zero-force baseline was determined by subsequent slackening of the fiber. Passive force was determined in the same manner at pCa 9.0 and was subtracted from the total force to obtain active force. Data were discarded if maximum Ca^{2+}-activated force in control conditions decreased more than 20% of the initial control. Force redevelopment kinetics (k_{TR}) were characterized by obtaining an apparent rate constant (expressed as reciprocal seconds) from the linear transformation of the half-time estimate ($t_{1/2}$) extrapolating from 50% to 63.2% ($k_{TR} = \tau^{-1} = -\ln 0.5 \times (t_{1/2})^{-1}$) (4,14). Monoexponential fits to the data, obtained with the Simplex method for nonlinear least-squares regression, gave similar results.

The relation between steady-state, active isometric force (F_{iso}) and pCa was fit to the Hill equation (Eq. 1) by nonlinear least-squares regression with Sigma Plot 2002 for Windows (version 8.0; SPSS, Chicago, IL).

$$\frac{F_{iso}}{F_0} = \frac{F_{max}/F_0}{\left(1 + 10^{n(pCa - pCa_{50})}\right)}, \quad (1)$$

where F_{max} is the maximum active force at saturating [Ca^{2+}] for a given condition, F_0 is the maximum force at saturating [Ca^{2+}] for ATP (i.e., $F_{max} = F_0$ for ATP), pCa_{50} is the pCa at which $F_{iso} = F_{max}/2$, and n is related to the steepness of the Ca^{2+} dependence around pCa_{50}.

Solutions

Relaxing and activating solutions were prepared as described previously (17,21) and contained 5 mM MgNTP (either ATP or dATP, or a combination of the two), 15 mM phosphocreatine, 1 mM P_i, 10 mM EGTA, 50 mM MOPS, 1 mM Mg^{2+}, 45 mM free Na^+, 100 mM free K^+, 1 mM DTT, and 200–400 units/ml creatine phosphokinase. Ca^{2+} solutions were prepared at evenly spaced pCa values ($pCa = -\log[Ca^{2+}]$, where [Ca^{2+}] is in molar) ranging from pCa 9 (relaxing) to pCa 5.0, plus pCa 4.5 (maximally activating). Intermediate pCa solutions were obtained by mixing prescribed volumes of the evenly spaced solutions. To alter solution [Ca^{2+}], appropriate amounts of $Ca(acetate)_2$ were added, taking into account desired free [Ca^{2+}] and the binding constants of all solutions constituents for Ca^{2+}. Ionic strength was maintained constant (180 mM) by varying Tris and acetate. Solution pH was adjusted to 7.0 at 12°C. Chemicals used in all experiments were supplied by Sigma-Aldrich (St. Louis, MO).

Diffusion-related radial NTP gradients were calculated as described previously (22) to estimate the magnitude of steady-state [NTP] gradients throughout the fiber bundle diameter. Calculations were made based on the radius of the largest fiber used for experiments (150 μm) and the concentration of total NTP (5 mM), NDP (~0.07 μM), and PCr (15 mM) in the fiber mechanics bathing solutions. These calculations were made assuming that CK activity was sufficient to maintain steady state throughout the fiber

bundle and that the Mg-NTPase rate was equivalent to that obtained in our solution actin-activated Mg-NTPase assays for dATP, since dATP was the faster rate. We also calculated the gradients using 2× the experimental dATPase rate to test the hypothetical case where Mg-NTPase rate in the intact sarcomere was larger than the measured solution Mg-NTPase rate. At 1× the dATPase rate, the final [dATP] at the center of the fiber was calculated to be ~5 mM, and the final [dADP] was ~5 μM. At 2× the dATPase rate, final [dATP] was ~5 mM and final [dADP] was ~14 μM. In absolute concentrations, these calculations represent an increase in [NDP] from $\ll$1 μM to ~10 μM. Thus both the concentration of NDP throughout even the largest diameter fiber bundles and particularly the correspondingly small gradients of NTP were considered negligible in these experiments.

In vitro motility assays

Solutions and flow cell preparation

IVM assays were performed to measure the sliding speed of fluorescently labeled F-actin over pcMyosin-coated surfaces. Experimental protocols, solution preparation, flow cell preparation, and analysis were essentially as described previously for rabbit skeletal HMM (23), with minor alterations for the pcMyosin preparation. Myosin concentration applied to motility flow cells was typically 0.15 mg/ml, which yielded smooth (nonerratic) motility of the actin filaments. In a subset of experiments, the concentration of pcMyosin was varied to alter the density of myosin on the flow cell surface (24). F-actin was fluorescently labeled with rhodamine phalloidin (RhPh). Assays were carried out at 30°C, with temperature in the flow cell maintained by an objective heating element (Temperature Controller B600; 20/20 Technology, Wilmington, NC); 0.1 M stocks of ATP and dATP were mixed in designated ratios of dATP/ATP. Immediately before the motility assay, 2 mM NTP (ATP, dATP, or a designated ratio of the two), 16.7 mM glucose, 100 μg/ml glucose oxidase, 18 μg/ml catalase (Worthington Biochemical, Lakewood, NJ), 0.3% methyl cellulose, and an additional 40 mM DTT were added to actin buffer (AB), composed of 25 mM KCl, 25 mM imidazole, 4 mM $MgCl_2$, 1 mM EGTA, 1 mM DTT, at pH 7.4 (25). Glucose, glucose oxidase, catalase, and extra DTT were added to minimize photobleaching of the RhPh label and photooxidative damage to the proteins (25,26).

Fluorescence microscopy and data acquisition

RhPh-labeled F-actin motility was observed by fluorescence microscopy on a Nikon Eclipse TE2000-U microscope (Nikon USA, Melville, NY) at 100× or 150× magnification, imaging five to six fields from varying areas on the flow cell. Field images were recorded as 30-s video clips using a VE1000SIT camera (Dage-MTI, Michigan City, IN) and a Sony RDR-GX7 DVD recorder. The DVD clips were processed using iMovie software as QuickTime files on a Macintosh 2X PowerPC G4 computer with a Miglia video interface (Miglia Technology, Enfield, UK). RhPh F-actin sliding speed distributions were analyzed by custom motion analysis software programs (designed by Thomas Asbury, P. Bryant Chase, and Nicolas Brunet, Florida State University). Briefly, individual filament speed was measured by tracking the centroids of filaments. A mean sliding speed for all filament paths (V_f) was calculated for each flow cell after removal of paths that had a ratio of mean ± SD path speed >0.3; this procedure effectively omits data from immobile filaments and filaments with erratic movement (23,26,27).

Actin-activated Mg-NTPase assays

Solutions

Actin-activated Mg-NTPase assays were performed as previously described (28) to measure the actin-activated rate of pcMyosin MgNTP hydrolysis in solution. Individual reactions were set up for each level of dATP/ATP in a microcentrifuge tube. Final reactions took place in a buffer of 1 mM DTT, 5 mM $MgCl_2$, 1 mM EGTA, 25 mM Tris (pH 7.0), and 0.05 M KCl, and utilized 0.2 mg/ml pcMyosin, 0.25 mg/ml F-actin, and 1 mM NTP (ATP, dATP, or a designated ratio of the two). Mg-NTPase reactions were stopped by addition of 13.3% SDS in 0.12 M EDTA, pH 7.0 (STOP solution), and indicator solution consisting of 0.5% ammonium molybdate (w/v), 0.5 M H_2SO_4, and 5 mg/ml ferrous sulfate.

Actin-activated Mg-NTPase activity

Timing of the assay began immediately upon addition of NTP; reactions were allowed to proceed with aliquots removed at indicated time points and dispensed directly into tubes containing STOP solution to terminate the reaction. Once all time points for each dATP/ATP ratio level were collected, indicator solution was added to each tube, and the tubes were incubated at 37°C for 15 min to allow color development. Absorbance was determined on a Beckman Coulter DU640 spectrophotometer (Beckman Coulter, Fullerton, CA) at 550 nm and converted to P_i concentration. Rate was based on the slope of the line obtained when P_i production was plotted against time, divided by the concentration of pcMyosin used in the assay. Mg-NTPase rate was determined for each dATP/ATP ratio level and plotted using linear regression with Excel (version 2000; Microsoft, Redmond, WA) or Sigma Plot 2002 for Windows (version 8.0; SPSS). Controls used in the assay included a negative NTP control with no NTP added, a negative ATP control with 100% ATP but no pcMyosin added, and a negative dATP control with 100% dATP but no pcMyosin added.

Data analysis and statistical analyses

All linear relationships (see Figs. 2–7) represent linear least-squares regressions. Statistical analyses for all experiments, including linear and nonlinear least-squares regression, were performed using Excel (version 2000; Microsoft) or Sigma Plot 2002 for Windows (version 8.0; SPSS). Where significance was applicable to fiber mechanics and IVM, the Student's *t*-test was used to compare means.

RESULTS

Steady-state force

Fig. 1 summarizes steady-state isometric Ca^{2+}-activated force in chemically permeabilized porcine cardiac papillary fiber bundles at either 5 mM ATP (*solid symbols*) or 5 mM dATP (*open symbols*). Passive force (pCa 9) was subtracted, and the resulting active force (F_{iso}) at each pCa was normalized to F_0 (pCa 4.5) for ATP for each individual fiber bundle. F_{iso} increased with dATP substituted for ATP at pCa levels between pCa 5.7 and pCa 4.5. The average maximal Ca^{2+}-activated force (F_{max}) at pCa 4.5 was 7.8 mN/mm^2. In this series of experiments, the data points show that F_{max} (pCa 4.5) was increased by ~9% with dATP as compared to ATP; at pCa 5.5, F_{iso} was increased by ~20% with dATP. Hill regression fits to these data indicate ~20% increase in F_{iso} at both pCa 4.5 and 5.5. Increases in F_{iso} found between ATP and dATP were smaller than those found in β-MHC rat (~39%, pCa 4.5; ~160%, pCa 5.5) (5). Force-pCa data were fit with the Hill equation (Eq. 1) to obtain estimates of pCa_{50} and n_H. We found no difference in pCa_{50} between ATP and dATP data in the porcine preparation, but we found overall higher Ca^{2+} sensitivity of force in the porcine preparation (Fig. 1; ATP, $pCa_{50} = 5.9 \pm 0.02$) as compared to

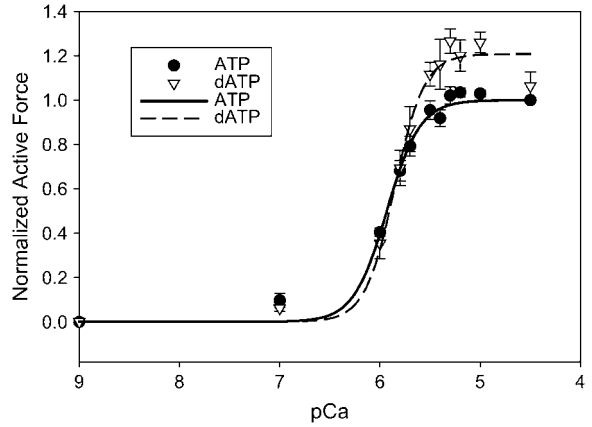

FIGURE 1 Force-pCa curves of skinned porcine papillary muscle utilizing 100% ATP (*solid circles*) or 100% dATP (*open triangles*) as the contractile substrate. Active force was normalized to F_{max} (pCa 4.5) for ATP in the same fiber bundle ($n = 7$). Lines are nonlinear least-squares regression fits to the Hill equation (Eq. 1). There were no differences in parameter estimates of pCa_{50} or n_H between ATP versus dATP.

previously published data from rat (ATP, $pCa_{50} = 5.43 \pm 0.01$) (5). There was no difference in n_H between ATP and dATP in the porcine preparation (Fig. 1).

In a separate set of experiments, we examined the steady-state force of the porcine cardiac papillary fiber bundles with increasing ratios of dATP/ATP at constant total NTP = 5 mM. Normalized data for pCa 4.5 and 5.5 are summarized in Fig. 2. The level of isometric force generally increased as the ratio of dATP/ATP was increased at both pCa levels. For this data set, overall force increases were ~8% for pCa 4.5, and ~35% for pCa 5.5 with 100% dATP compared to ATP. At

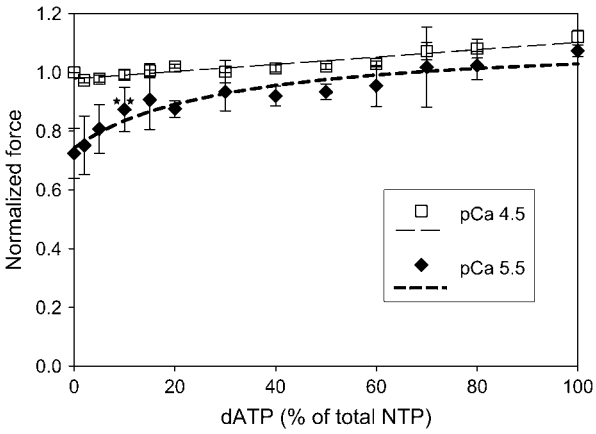

FIGURE 2 The relationship between isometric force and dATP/ATP ratio. Isometric force increases linearly with dATP/ATP ratio at pCa 4.5 (*open squares*) and nonlinearly at pCa 5.5 (*solid diamonds*). Active force was normalized to F_{max} for ATP ($n = 5$–7). Lines are the linear least-squares regression (pCa 4.5) or nonlinear least-squares regression fit to Eq. 2 (pCa 5.5). Regression analysis suggests approximately fourfold higher affinity of dATP for cardiac myosin than ATP at pCa 5.5 (Eq. 2). (**$p < 0.01$ at 10% dATP).

submaximal Ca^{2+} activation (pCa 5.5), there was a highly significant increase in the F_{iso} at 10% dATP ($p < 0.01$), where force was increased by ~20%.

At pCa 4.5, the relationship between normalized force and dATP/ATP was essentially linear (Fig. 2). Interestingly, at pCa 5.5, the relationship was clearly nonlinear (Fig. 2). At dATP/ATP ratios between 2 and 20% the slope was higher than between 20 and 100%, indicating high increases in steady-state force as the proportion of dATP was increased by a small amount and smaller, linear increases in force as the proportion of dATP was increased further. The nonlinear relation between F_{iso} at pCa 5.5 and dATP/ATP was fit by nonlinear regression to a modified mixed alternative substrates equation (29), (alternative substrates were ATP or dATP).

$$\frac{F_{iso}}{F_0} = \frac{f_A\dfrac{[ATP]}{K_{m_{ATP}}} + f_{dA}\dfrac{[dATP]}{z \times K_{m_{ATP}}}}{1 + \dfrac{[ATP]}{K_{m_{ATP}}} + \dfrac{[dATP]}{z \times K_{m_{ATP}}}}, \quad (2)$$

where F_{iso}/F_0 is the normalized force at any given ratio of [dATP]/[ATP], f_A and f_{dA} represent force for 100% ATP or 100% dATP at each Ca^{2+} level, K_m is the K_m of ATP for myosin fixed at 2.3 μM (30), and z represents the factor by which the K_m of dATP differs from that of ATP ($K_{mdATP} = z \times K_{mATP}$). Regression parameter $z = 0.23 \pm 0.09$ (Eq. 2) at pCa 5.5, implying that the apparent affinity of dATP for pcMyosin is approximately fourfold higher than that of ATP, although this may not be the only mechanistic explanation for the nonlinearity.

Rate of force redevelopment (k_{TR})

The kinetics of tension redevelopment (k_{TR}) is an indicator of the kinetics of strong cross-bridge attachment and detachment (31) and varies with Ca^{2+} concentration (18,32–34). Attachment/detachment kinetics determine actomyosin duty ratio, which in turn is a primary determinant of the number of strongly bound cross-bridges and therefore total isometric force. A change in the number of strong cross-bridges via altered duty ratio could further alter the number of strong cross-bridges via an effect on cooperative activation of the thin filament (6). Fig. 3 summarizes the Ca^{2+} dependence of k_{TR} in porcine cardiac papillary muscle with either 100% ATP or dATP as substrate. For each fiber, k_{TR} values were normalized to that obtained with ATP at pCa 4.5. At each level of Ca^{2+} activation, dATP increased the rate of tension redevelopment over that achieved with ATP. These data differ somewhat from previous rat trabeculae data, where dATP did not affect k_{TR} at the lowest levels of Ca^{2+} activation (5). Fig. 3 also shows that with either ATP or dATP there was little variation of k_{TR} with [Ca^{2+}]. This contrasts with k_{TR} effects seen in faster muscle types (4,5). When normalized k_{TR} was plotted against normalized steady-state

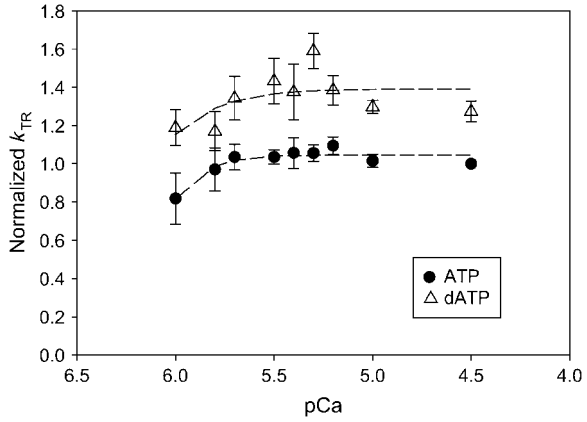

FIGURE 3 Faster kinetics of tension redevelopment (k_{TR}) with 100% dATP (*open triangles*) over 100% ATP (*solid circles*) at all levels of Ca^{2+} activation ($n = 7$). k_{TR} was normalized to that at pCa 4.5 with ATP (0.34 ± 0.009 s^{-1}). Although there was little variation of k_{TR} with calcium concentration for either dATP or ATP, k_{TR} was faster with dATP for all levels of Ca^{2+} activation.

isometric force measured before the release-restretch maneuver (Fig. 4), we found that k_{TR} was faster with dATP at all force levels. In a separate set of experiments, we determined k_{TR} as the ratio of dATP/ATP was varied from 100% ATP to 100% dATP. Fig. 5 shows that at both pCa 4.5 (maximum Ca^{2+} activation) and pCa 5.5, there was a linear increase in k_{TR} as the dATP/ATP ratio was increased.

Actin-activated Mg-NTPase

We utilized an actin-activated Mg-NTPase assay to investigate the differences in the rates of nucleotide hydrolysis for varying ratios of dATP/ATP under unloaded conditions with pcMyosin. Fig. 6, *A* and *B*, shows the data obtained from one

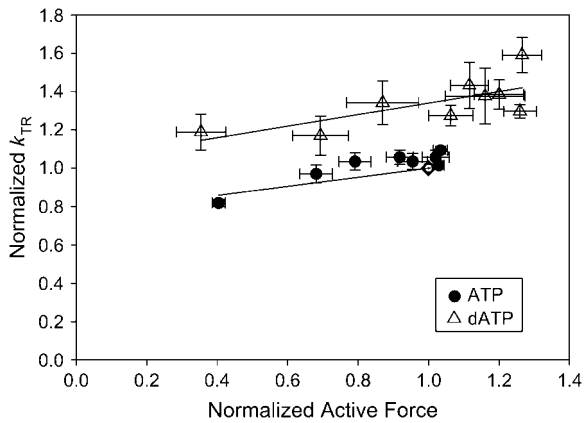

FIGURE 4 The relationship between steady-state force and k_{TR} with ATP (*solid circles*) or dATP (*open triangles*). The data from Figs. 1 and 3 were binned by pCa. k_{TR} and force were normalized to that at pCa 4.5 with ATP (*open diamond*). Lines represent linear least-squares regressions on the data. k_{TR} was higher with dATP at all levels of Ca^{2+} activation.

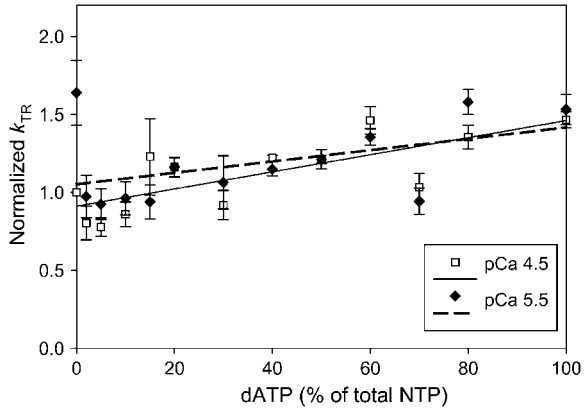

FIGURE 5 Linear relationship between k_{TR} and dATP/ATP ratio at both pCa 4.5 (*open squares*) and pCa 5.5 (*solid diamonds*). Lines represent linear least-squares regressions on the data. k_{TR} was normalized to that at pCa 4.5 with ATP ($n = 5$–7).

representative experiment, and similar results were achieved in three independent experiments. We found a linear relationship between the rate of NTP hydrolysis and increasing ratio of dATP/ATP, where hydrolysis increased as much as 27% when dATP was completely substituted for ATP as substrate in the assay.

In vitro motility

We utilized the unregulated IVM to examine unloaded filament sliding and, as with the Mg-NTPase assays, investigate cross-bridge cycling without the effects of internal loads that are present in fiber bundle preparations. This assay measures the sliding speed of RhPh F-actin (V_f) as it interacts with pcMyosin that is bound to the nitrocellulose-coated surface of a coverslip (Methods) and gives insight into the kinetics of the release step in the actomyosin cross-bridge cycle. The data points presented in Fig. 7 show that V_f increased by ~47% when ATP was replaced with dATP. There was an overall linear increase in V_f as the dATP/ATP ratio was increased. We found a highly significant increase in V_f at 10% dATP/ATP, corresponding with the ratio at which significance was found in our steady-state force data.

To determine if the quality of the motility observed with the IVM assay could provide some directly observable insight into the effect of dATP cross-bridges on actomyosin interaction, flow cells with varying pcMyosin densities (Methods) were examined using either ATP or dATP in the motility assay. Fig. 8 shows that the filaments at low pcMyosin densities (<0.075 mg/ml) were very long and as indicated in the 30-s filament position tracking, were primarily immobile for both ATP and dATP. When dATP was utilized as substrate, optimal filament sliding was achieved at a lower pcMyosin density than with ATP. At the midrange, optimal motility densities (between 0.075 and 0.15 mg/ml) there was a highly significant increase in V_f with dATP over

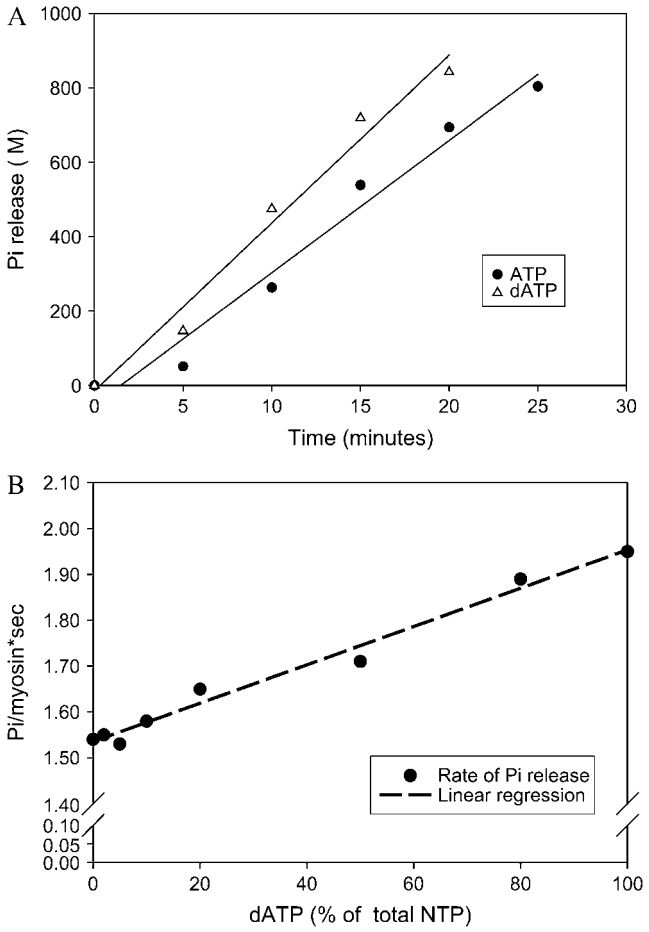

FIGURE 6 Data from representative assays of unregulated actin-activated Mg-NTPase activity of pcMyosin. (*A*) Linear time course of P_i release for ATP hydrolysis (100% ATP; *solid circles*) or dATP hydrolysis (100% dATP; *open triangles*). Conditions were as described in Methods. (*B*) Linear dependence of NTP hydrolysis rate on dATP/ATP ratio. Each point is derived from the slope of a time course of P_i production as shown in panel *A* (values from *A* correspond to the highest and lowest values on the abscissa). Lines represent linear least-squares regressions on the data.

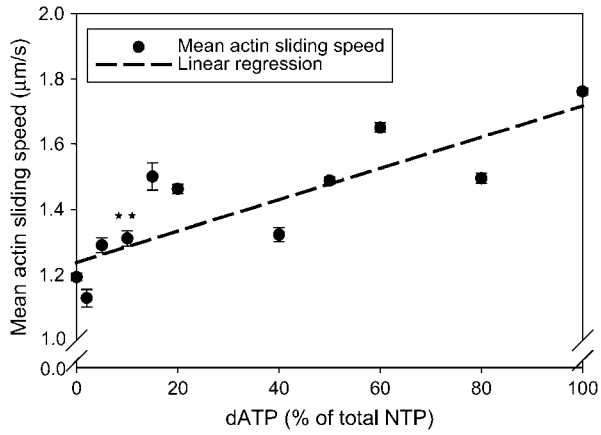

FIGURE 7 Linear dependence of unregulated actin sliding speed in the IVM assay on dATP/ATP ratio. Conditions for motility assays with pcMyosin were as described in Methods. Each point is the mean ± SE of speed from ≥150 filament paths per flow cell measured in 3–8 flow cells per level (**$p < 0.01$ at 10% dATP). Line represents linear least-squares regressions on the data.

that with ATP (data not shown); filaments were of moderate length, and most of the filaments were uniformly motile over the 30-s time frame (Fig. 8). Motility at high densities (>0.15 mg/ml) was qualitatively quite different; filaments were sheared apart and measured actin sliding speed decreased with increase in pcMyosin density. Many filaments were immobile, whereas those that did move had very short filament paths over the 30-s time frame (Fig. 8). This drop-off in motility quality quickly declined at 0.2 mg/ml with dATP in contrast to ATP, where optimal motility could still be maintained at 0.2 mg/ml pcMyosin density. Presumably with an increase in the overall number of myosin heads on the surface, there was a corresponding increase in the number of ''dead heads'' that can hold filaments immobile. Because more cross-bridges form at a faster on rate with dATP as substrate at a given myosin density, there is a shearing effect, resulting in an increase in the breakage of actin filaments at a lower pcMyosin density (above optimal) with dATP than ATP and an overall decrease in quality of motility. These qualitative observations are consistent with dATP causing increased numbers of strongly bound actomyosin cross-bridges.

DISCUSSION

Replacement of ATP by dATP as contractile substrate for rat cardiac muscle may cause an increase in the number of strongly attached cross-bridges, which in turn activates the cardiac thin filament to a level over that achievable with ATP and saturating Ca^{2+} (1,5). On that basis, porcine cardiac muscle was used to determine if a low dATP/ATP ratio could significantly enhance experimental indicators of contraction in vitro and also to increase our understanding of the mechanism by which dATP has a direct effect on the actomyosin duty cycle during contraction. Porcine cardiac muscle was examined because it contains a β-MHC isoform that is kinetically similar to human (10). The two major findings of our study are as follows: i), there is a significant enhancement of in vitro contractile parameters when only 10% of the total ATP substrate available to pcMyosin is substituted with dATP (Figs. 2 and 7); and ii), involvement of dATP as substrate for the actomyosin cycle causes faster cycling and a higher duty ratio, increased activation of the thin filament at high Ca^{2+}, and overall enhanced contractility primarily via increased numbers of strong, force-producing cross-bridges.

Partial replacement of ATP with dATP

We find a significant enhancement of several parameters of cardiac contraction when only 10% of ATP available for

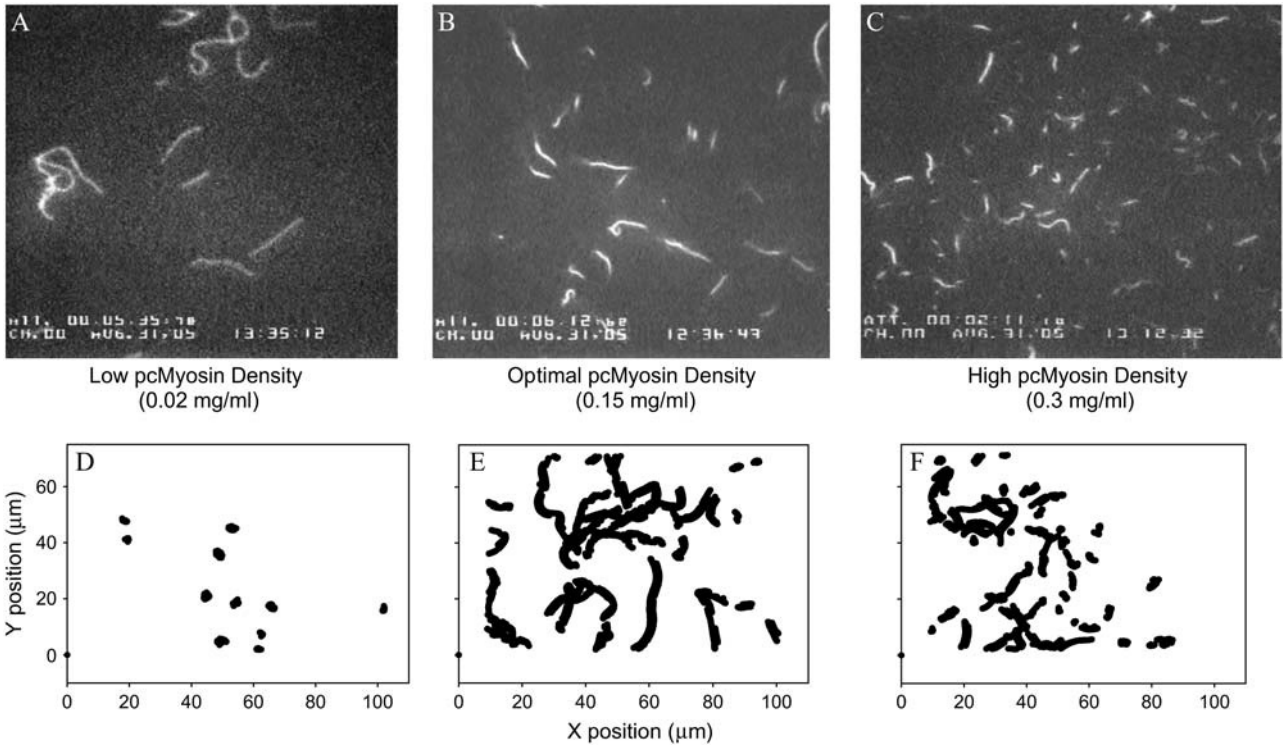

FIGURE 8 Representative data from motility assays at different surface densities of pcMyosin. Single video frames (*A–C*) and centroid analysis (*D–F*) were from assays conducted after applying (*A*, *D*) 0.02 mg/ml pcMyosin, (*B*, *E*) 0.15 mg/ml pcMyosin, or (*C*, *F*) 0.3 mg/ml pcMyosin. Panels *D–F* represent the superposition of centroids of all actin filaments over a 30-s time period that includes the frames shown in panels *A–C*. Little progressive motility is indicated at low (*D*) and high (*F*) densities by very small changes in centroid position over time. Progressive motility is indicated at optimal density (*E*) by continuous lines (superimposed time series). Very short filaments are evidence for shearing of actin filaments at high pcMyosin densities (*C*).

actomyosin interaction is replaced with dATP (Figs. 2 and 7). To determine if substitution of a small percentage of ATP with dATP could achieve a significant enhancement of steady-state force in porcine cardiac papillary muscle, we tested F_{iso} at pCa 4.5 and 5.5 with increasing ratios of dATP/ATP (constant total NTP). The ~20% increase in force found at pCa 5.5 with 10% dATP (90% ATP) was highly significant ($p < 0.01$, Student's *t*-test). Similarly, actomyosin interactions under unloaded conditions were examined using the unregulated IVM assay as the ratio of dATP/ATP (constant total NTP) was increased in the motility buffer. A 10% dATP/ATP ratio resulted in a 10% increase in actin sliding speed (Fig. 7), which was also highly significant. Actin-activated Mg-NTPase results followed this same general trend (Fig. 6 *B*), although a significant increase from 0% to 10% dATP/ATP could not be determined from the three data sets obtained. We therefore conclude that if only 10% of the ATP available to cardiac myosin was converted to dATP, there would be a functionally significant enhancement of overall cardiac contractility.

With our in vitro assays, partial replacement of ATP with dATP resulted in a linear relationship between each parameter measured and dATP/ATP ratio. This linear relationship occurred almost independently of what type of measurement was made—whether regulated or unregulated conditions, isometric or unloaded conditions, or dynamic (kinetic) conditions. F_{max} (Fig. 2, pCa 4.5) increases linearly under regulated, isometric conditions. In Fig. 5, the same linear relationship is found for k_{TR} at both pCa 4.5 and 5.5 under regulated and pseudoisometric conditions. The unregulated, unloaded kinetic measurements of actin-activated Mg-NTPase and actin filament sliding speed (Figs. 6 *B* and 7) with increasing replacement of ATP with dATP increased the measured parameters linearly. Explanation of these observations, along with the pCa_{50} and n_H derived from the force-pCa data (Fig. 1), does not require additional thin filament activation when dATP is utilized as contractile substrate instead of ATP. The porcine data differ from the rat data where dATP increased Ca^{2+} sensitivity of force, although in both cases there was no significant effect on n_H (5).

Although most of our data suggest no increased activation of the thin filament when dATP is contractile substrate, the nonlinear relationship between force and dATP/ATP ratio at pCa 5.5 (Fig. 2) may indicate otherwise. Together with the force-pCa data (Fig. 1), this nonlinearity may be explained as enhanced activation of the thin filament proteins, but only at high calcium levels (pCa $\leq$ 5.7). At these calcium levels, the cooperativity of increased numbers of cross-bridges may cause enhanced activation of the thin filament, resulting in a steep, nonlinear relationship at the lower dATP/ATP ratios

between 2 and 20%. At some point, enhanced thin filament activation reaches a maximum, so that as the number of strongly attached cross-bridges increases with increasing dATP/ATP ratio, the thin filament activation enhancement that can be achieved does not dominate in force generation. At this point the increasing number of strongly attached cross-bridges becomes dominant in force generation, thus the curve reflects a linear increase between 20 and 100% dATP (Fig. 2). Although we consider this to be the most likely explanation for the observed nonlinearity, there is another factor that may contribute to the overall effect. The mixed alternative substrate equation used to analyze this data (Eq. 2) allows for the K_m of ATP for pcMyosin to be fixed at the value measured in rabbit skeletal muscle (30) and the K_m of dATP for pcMyosin to vary. Using this model, our results were consistent with the K_m of dATP for pcMyosin being lower than that of ATP by approximately fourfold (Results). If this interpretation is correct, then higher affinity for dATP could also contribute to faster cycling with an increase in the detachment rate as dATP binds pcMyosin. In either case, an increase in the number of cross-bridges would contribute to an increase in force.

Effects of dATP on actomyosin kinetics

In addition to increased thin filament activation, increased isometric force could result from increased actomyosin duty ratio (the steady-state fraction of actomyosin cross-bridges that turn over in the force generating state). The duty ratio has been defined (31) as α_{Fs} where

$$\alpha_{F_s} = \frac{f_{app}}{f_{app} + g_{app}}. \quad (3)$$

f_{app} is the transition from nonforce generating states to force generating states and is representative of the attachment phase of the cross-bridge cycle, and g_{app} is the transition from force generating states to nonforce generating states and is representative of the detachment phase of the cycle. g_{app} may represent g_1 for isometric conditions or g_2 ($g_2 > g_1$) for unloaded conditions (35). We found that F_{iso} was increased with dATP substituted for ATP at pCa levels between 5.7 and 4.5 with porcine cardiac muscle (Fig. 1) and is indicative of an increase in α_{Fs}. This is in agreement with observations in rat cardiac muscle (5), but only at pCa $\leq$ 5.7. At low Ca^{2+} levels (pCa $\geq$ 6) there was no detectable increase in force for the pig preparation, presumably due to species differences in Tn and Tm isoforms. If isometric force as reflected by the duty ratio is increased (Eq. 3), then either f must increase and/or g_1 must decrease; alternatively, if g_1 increases, then a proportionally greater increase in f must also occur to obtain an increase in the duty ratio.

The unloaded kinetics of actomyosin cross-bridge detachment with dATP as contractile substrate was examined with unregulated actin sliding speed and unregulated actin-activated Mg-NTPase. An increased sliding speed with dATP indicates an increase in g_2. Our results (Figs. 7 and 8) support an increase in actual numbers of interacting cross-bridges when dATP is utilized as substrate in the actomyosin cross-bridge cycle. The ~47% increase in sliding speed when dATP completely replaces ATP as substrate indicates an increase in the detachment rate of the actomyosin duty cycle, contributing to overall shortening of the cycle (Fig. 9). Likewise, the increased Mg-NTPase rate found with dATP as substrate (Fig. 6) is consistent with an increase in g_2. Because the rate-limiting step of NTP hydrolysis occurs when myosin is detached from actin, an increase in the Mg-NTPase rate results in an overall decrease in total cycling time. The Mg-NTPase results can most simply be interpreted as an increase in g_2, but there is an alternative explanation that cannot be ruled out. The methodology employed to measure the actin-activated Mg-NTPase rate directly measured the P_i release rate; therefore an increase in Mg-NTPase rate with dATP could also reflect increased numbers of cycling cross-bridges. This would mean that the affinity of actin for myosin increases when dATP is involved in hydrolysis. Previous work compared the Mg-NTPase rate with increasing concentration of F-actin, utilizing either dATP or ATP as substrate for hydrolysis (1). The data indicated a 53% increase in V_{max} when dATP was utilized rather than ATP and a slight decrease in the K_m of myosin for actin with dATP as substrate. This suggests that at least some of the increased Mg-NTPase rate with dATP utilized as substrate for pcMyosin (Fig. 6) could be due to an increased number of cycling cross-bridges, but much of the rate increase is due to a decrease in actomyosin cycle time (Fig. 9).

With porcine cardiac papillary muscle, we found that k_{TR} was increased with dATP over ATP at all levels of Ca^{2+} activation (Fig. 3). Previous rat data indicated that dATP increased k_{TR} only at higher levels of Ca^{2+} activation (5). The difference in our results can most likely be attributed to differences in the species isoforms of thin filament regulatory proteins. We find an increase in k_{TR} at all levels of Ca^{2+}-activated force generation, and high k_{TR} rates correspond

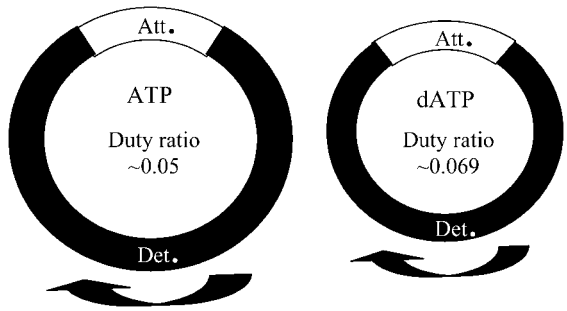

FIGURE 9 Comparison of the actomyosin cycle in cardiac contraction for ATP (*left*) versus dATP (*right*). The entire actomyosin cross-bridge cycle is shorter with dATP due to an increase in the attachment and detachment rates, as well as overall faster NTP hydrolysis rate during the detached phase (*Det*). The percentage of the total attached time (*Att*) during the cycle increases, resulting in a higher isometric duty ratio for dATP than ATP.

with forces that are above that achievable with ATP at F_{max} (Fig. 4). This result is in agreement with previous rat data (5) and provides additional evidence that dATP-induced binding of higher numbers of strong cross-bridges results in higher force due to an enhancement of thin filament activation beyond ATP maximum calcium activation. k_{TR} is defined as $k_{TR} = f + g_1$ (32) and thus reflects both attachment and detachment rates. An elevation of k_{TR} at all levels of Ca^{2+}-activated force (Fig. 4) indicates that g_1 is faster with dATP than ATP (4,33). This is in agreement with the observed increase in g_2 (Figs. 6 and 7). The overall increase in k_{TR} indicates that the rate of strong cross-bridge detachment and attachment are both enhanced when dATP is utilized as contractile substrate; both rates contribute to the overall shortening of the entire actomyosin cycle and an increased α_{Fs} for dATP over ATP (Fig. 9).

Mechanisms of dATP's effect on contractility

Our data and others' data (1–3,5) suggest that part of dATP's effect on contractility is due to increased number of cross-bridges when dATP is utilized as substrate for actomyosin kinetics rather than ATP. Fig. 4 indicates that dATP promotes both higher force and k_{TR} above that achievable with ATP at maximum Ca^{2+} activation. This has been described by Regnier et al. with rat trabeculae as enhanced thin filament activation via higher numbers of bound cross-bridges with dATP (5). Our kinetic data, however, add some additional insight into the mechanisms of dATP's contractile enhancement. Our data indicate a higher affinity of pcMyosin for dATP than for ATP that was observable with partial replacement of ATP with dATP at pCa 5.5 (Fig. 2). Faster k_{TR} with increased isometric force indicates a faster attachment rate as myosin and actin interact to enter into the attached, force-producing phase. Our IVM, Mg-NTPase, and k_{TR} data indicate a faster detachment rate of myosin from actin when dATP is substrate. The combination of a faster attachment rate (f) as well as a faster detachment rate (g) results in a higher duty ratio if a proportionally greater increase in f occurs. In addition, the detached phase is shortened, as evidenced by the faster Mg-NTPase. We infer that the actual amount of time that cross-bridges remain in the attached phase with dATP may be somewhat shorter than that for ATP, there is a greater shortening of the overall actomyosin cycle and thus the isometric duty ratio is actually higher with dATP than with ATP (Fig. 9). This higher duty ratio is reflected in the significant increase of isometric force that is achieved with dATP as substrate.

Although the normal physiological ratio of dATP/ATP is $\ll 1$ (36), our finding that $\sim$10% dATP/ATP can significantly increase many aspects of cardiac contractility in vitro has potential implications for modulation of cardiac function. These increases are caused by an increased number of strongly attached, force-producing cross-bridges that further activate the thin filament and result in a shorter actomyosin cross-bridge cycle with a higher duty ratio when dATP is used as contractile substrate rather than ATP. The direct effect that dATP has on actomyosin interaction and cardiac contractility makes exploration of methods for increasing intracellular cardiac dATP/ATP ratios attractive. If feasible, dATP may have possibilities as a candidate for positive inotropic therapy for the symptoms of heart failure.

We express our gratitude to Lori McFadden for preparation of actin, Victor Miller for help in performing IVM experiments, John Williams for help in acquiring porcine hearts, and Bradley's Country Store for providing the porcine hearts.

This work was supported by National Institutes of Health grant NIH-NHLBI HL63974 and a predoctoral fellowship (B.S.) from Florida State University's Center for Materials Research and Technology (MARTECH).

REFERENCES

1. Regnier, M., A. J. Rivera, Y. Chen, and P. B. Chase. 2000. 2-deoxy-ATP enhances contractility of rat cardiac muscle. *Circ. Res.* 86:1211–1217.
2. Regnier, M., and E. Homsher. 1998. The effect of ATP analogs on posthydrolytic and force development steps in skinned skeletal muscle fibers. *Biophys. J.* 74:3059–3071.
3. Regnier, M., D. M. Lee, and E. Homsher. 1998. ATP analogs and muscle contraction: mechanics and kinetics of nucleoside triphosphate binding and hydrolysis. *Biophys. J.* 74:3044–3058.
4. Regnier, M., D. A. Martyn, and P. B. Chase. 1998. Calcium regulation of tension redevelopment kinetics with 2-deoxy-ATP or low [ATP] in rabbit skeletal muscle. *Biophys. J.* 74:2005–2015.
5. Regnier, M., H. Martin, R. J. Barsotti, A. J. Rivera, D. A. Martyn, and E. Clemmens. 2004. Cross-bridge versus thin filament contributions to the level and rate of force development in cardiac muscle. *Biophys. J.* 87:1815–1824.
6. Gordon, A. M., E. Homsher, and M. Regnier. 2000. Regulation of contraction in striated muscle. *Physiol. Rev.* 80:853–924.
7. Fitzsimons, D. P., J. R. Patel, and R. L. Moss. 2001. Cross-bridge interaction kinetics in rat myocardium are accelerated by strong binding of myosin to the thin filament. *J. Physiol.* 530:263–272.
8. Clemmens, E. W., and M. Regnier. 2004. Skeletal regulatory proteins enhance thin filament sliding speed and force by skeletal HMM. *J. Muscle Res. Cell Motil.* 25:515–525.
9. Houser, S. R., and K. B. Margulies. 2003. Is depressed myocyte contractility centrally involved in heart failure? *Circ. Res.* 92:350–358.
10. Malmqvist, U. P., A. Aronshtam, and S. Lowey. 2004. Cardiac myosin isoforms from different species have unique enzymatic and mechanical properties. *Biochemistry.* 43:15058–15065.
11. Schoffstall, B., A. Clark, and P. B. Chase. 2005. Increasing ratios of 2-dATP/ATP linearly enhances isometric force of porcine cardiac papillary muscle. *J. Mol. Cell. Cardiol.* 38:817.
12. Schoffstall, B., Clark, A., and Chase, P. B. 2005. Porcine cardiac muscle contractility is enhanced by increasing ratios of 2-dATP/ATP. *Circ. Res.* 97:199 (online suppl. page e-42).
13. Pardee, J. D., and J. A. Spudich. 1982. Purification of muscle actin. *Methods Enzymol.* 85:164–181.
14. Schoffstall, B., A. Kataoka, A. Clark, and P. B. Chase. 2005. Effects of rapamycin on cardiac and skeletal muscle contraction and crossbridge cycling. *J. Pharmacol. Exp. Ther.* 312:12–18.
15. Gomes, A. V., G. Venkatraman, J. P. Davis, S. B. Tikunova, P. Engel, R. J. Solaro, and J. D. Potter. 2004. Cardiac troponin T isoforms affect the $Ca^{(2+)}$ sensitivity of force development in the presence of slow skeletal troponin I: insights into the role of troponin T isoforms in the fetal heart. *J. Biol. Chem.* 279:49579–49587.

16. Palmiter, K. A., M. J. Tyska, J. R. Haeberle, N. R. Alpert, L. Fananapazir, and D. M. Warshaw. 2000. R403Q and L908V mutant beta-cardiac myosin from patients with familial hypertrophic cardiomyopathy exhibit enhanced mechanical performance at the single molecule level. *J. Muscle Res. Cell Motil.* 21: 609–620.

17. Chase, P. B., and M. J. Kushmerick. 1988. Effects of pH on contraction of rabbit fast and slow skeletal muscle fibers. *Biophys. J.* 53: 935–946.

18. Chase, P. B., D. A. Martyn, and J. D. Hannon. 1994. Isometric force redevelopment of skinned muscle fibers from rabbit activated with and without Ca^{2+}. *Biophys. J.* 67:1994–2001.

19. Regnier, M., A. J. Rivera, C. K. Wang, M. A. Bates, P. B. Chase, and A. M. Gordon. 2002. Thin filament near-neighbour regulatory unit interactions affect rabbit skeletal muscle steady-state force-$Ca^{(2+)}$ relations. *J. Physiol.* 540:485–497.

20. Chase, P. B., D. A. Martyn, and J. D. Hannon. 1994. Activation dependence and kinetics of force and stiffness inhibition by aluminiofluoride, a slowly dissociating analogue of inorganic phosphate, in chemically skinned fibres from rabbit psoas muscle. *J. Muscle Res. Cell Motil.* 15:119–129.

21. Martyn, D. A., and A. M. Gordon. 1988. Length and myofilament spacing-dependent changes in calcium sensitivity of skeletal fibres: effects of pH and ionic strength. *J. Muscle Res. Cell Motil.* 9: 428–445.

22. Chase, P. B., and M. J. Kushmerick. 1995. Effect of physiological ADP concentrations on contraction of single skinned fibers from rabbit fast and slow muscles. *Am. J. Physiol.* 268:C480–C489.

23. Chase, P. B., Y. Chen, K. L. Kulin, and T. L. Daniel. 2000. Viscosity and solute dependence of F-actin translocation by rabbit skeletal heavy meromyosin. *Am. J. Physiol. Cell Physiol.* 278:C1088–C1098.

24. Uyeda, T. Q., S. J. Kron, and J. A. Spudich. 1990. Myosin step size. Estimation from slow sliding movement of actin over low densities of heavy meromyosin. *J. Mol. Biol.* 214:699–710.

25. Kron, S. J., Y. Y. Toyoshima, T. Q. Uyeda, and J. A. Spudich. 1991. Assays for actin sliding movement over myosin-coated surfaces. *Methods Enzymol.* 196:399–416.

26. Gordon, A. M., M. A. LaMadrid, Y. Chen, Z. Luo, and P. B. Chase. 1997. Calcium regulation of skeletal muscle thin filament motility in vitro. *Biophys. J.* 72:1295–1307.

27. Sellers, J. R., G. Cuda, F. Wang, and E. Homsher. 1993. Myosin-specific adaptations of the motility assay. *Methods Cell Biol.* 39:23–49.

28. White, H. D. 1982. Special instrumentation and techniques for kinetic studies of contractile systems. *Methods Enzymol.* 85:698–708.

29. Segel, I. H. 1993. Enzyme Kinetics: Behaviour and Analysis of Rapid Equilibrium and Steady-State Enzyme Systems. John Wiley & Sons, New York.

30. Cooke, R., and W. Bialek. 1979. Contraction of glycerinated muscle fibers as a function of the ATP concentration. *Biophys. J.* 28:241–258.

31. Brenner, B., and E. Eisenberg. 1986. Rate of force generation in muscle: correlation with actomyosin ATPase activity in solution. *Proc. Natl. Acad. Sci. USA.* 83:3542–3546.

32. Brenner, B. 1988. Effect of Ca^{2+} on cross-bridge turnover kinetics in skinned single rabbit psoas fibers: implications for regulation of muscle contraction. *Proc. Natl. Acad. Sci. USA.* 85:3265–3269.

33. Regnier, M., A. J. Rivera, P. B. Chase, L. B. Smillie, and M. M. Sorenson. 1999. Regulation of skeletal muscle tension redevelopment by troponin C constructs with different Ca^{2+} affinities. *Biophys. J.* 76:2664–2672.

34. Sweeney, H. L., and J. T. Stull. 1990. Alteration of cross-bridge kinetics by myosin light chain phosphorylation in rabbit skeletal muscle: implications for regulation of actin-myosin interaction. *Proc. Natl. Acad. Sci. USA.* 87:414–418.

35. Huxley, A. F. 1957. Muscle structure and theories of contraction. *Prog. Biophys. Biophys. Chem.* 7:255–318.

36. Traut, T. W. 1994. Physiological concentrations of purines and pyrimidines. *Mol. Cell. Biochem.* 140:1–22.